J Med Ultrasonics (2005) 32:39–47
DOI 10.1007/s10396-005-0034-2

ORIGINAL ARTICLE

Kazuhiro SUNAGAWA · Hiroshi KANAI

Measurement of shear wave propagation and investigation of estimation of shear viscoelasticity for tissue characterization of the arterial wall

Received: August 20, 2004 / Accepted: November 16, 2004

Abstract
Purpose. The aim of this study was to find an array of frequency components, ranging from 0 Hz (direct current) to several tens of hertz that comprise the small vibrations on the arterial wall using noninvasive in vivo experiments. These vibrations are caused mainly by blood flow. The viscoelasticity of the arterial wall was estimated from the frequency characteristics of these vibrations propagating from the intima to the adventitia.
Methods. Propagation of these frequencies in human tissue displays certain frequency characteristics. Based on the Voigt model, shear viscoelasticity can be estimated from the frequency characteristics of the propagating vibrations. Moreover, we estimated shear viscoelasticity from the measured frequency characteristics of shear wave attenuation.
Results. Shear wave propagation from the intima to the adventitia resulting from blood flow was explained theoretically based on the obtained measurements. Shear viscoelasticity was also estimated from the measured frequency characteristics of shear wave attenuation.
Conclusions. Based on the proposed method, shear viscoelasticity can be estimated from ultrasonographic measurements. These results have a novel potential for characterizing tissue noninvasively.

Keywords phased tracking method · shear viscoelasticity · shear wave · tissue characterization · ultrasound

K. Sunagawa · H. Kanai (✉)
Department of Electronic Engineering, Graduate School of Engineering, Tohoku University, Aramaki-aza-Aoba 05, Aoba-ku, Sendai 980-8579, Japan
Tel. +81-22-795-7078; Fax +81-22-263-9444
e-mail: hkanai@ecei.tohoku.ac.jp

K. Sunagawa
Panasonic Mobile Communications Sendai R&D Laboratory, Sendai, Japan

Introduction

Changes in blood pressure are produced by cardiac pulses propagated as pulse waves from the heart to the arterial periphery, causing the arterial wall to vibrate at frequencies of up to tens of hertz. Palpation can also be used to check pulsation in the radial and other arteries. Because pulse wave velocity varies with the elasticity and viscosity of the arterial wall, several methods for evaluating wall elasticity[1,2] and viscosity[3–5] based on pulse wave velocity have been proposed.

The smooth muscles constituting the arterial wall contract or relax when stimulated by vasoactive substances.[6] For example, sublingual administration of nitroglycerin, a vasoactive agent, causes the smooth muscles of the arteries to relax. Chronologic ultrasound analysis of changes in arterial wall thickness showed that smooth muscle response to sublingual nitroglycerin appeared several tens of seconds after the dose was administered, and that wall thickness changed slowly over a period of several tens of seconds after the first signs of response.

Pulsation of the heart also produces turbulent blood flow or eddies within the arterial lumen that express themselves as murmurs at a frequency range higher than that of the pulse waves. We measured human carotid artery small vibration on the atrial wall percutaneously using a phased tracking method capable of precisely measuring small vibration of the arterial wall with ultrasonography.[7,8] Vibration of the arterial wall contained direct current and alternating current components at frequencies up to slightly higher than 100 Hz.[9,10]

Local changes in stress on the surface of the arterial wall produced by disturbances in blood flow or formation of eddies appears to be a factor accounting for this small vibration. Vibration of the arterial wall also appears to propagate from the intima to the adventitia, and local stress changes on the arterial wall surface appear to produce vibration. Similarly, the propagation characteristics of vibration from the surface of the arterial wall vary with viscoelasticity characteristics of the tissue constituting the wall.

Methods for evaluating viscoelasticity based on analysis of vibration propagation characteristics through tissue after vibration of the living tissue by external excitation have been proposed.[11–14] However, because these methods require an external source of vibration and a system for measuring the internal vibration produced, they also expose the subject to greater stress. Furthermore, these methods introduce another problem by causing the entire blood vessel to bend when the arterial wall is vibrated in this way. To avoid these complications, we used a source of vibration inherent in the living body and estimated the viscoelasticity of living tissue in a simple, noninvasive manner.

We propose a new method for estimating tissue viscoelasticity based on the assumption that arterial wall tissue serves as a Voigt model in which Hooke's law is applicable. Tissue viscoelasticity is thus estimated based on the frequency characteristics of the attenuation of arterial wall vibration, probably induced by blood flow as it propagates from the intima to the adventitia. This frequency ranges from direct current to tens of hertz.

This method does not require measuring the stress applied to the elastic body, as do conventional methods of estimating viscoelasticity. Furthermore, because it uses vibration occurring naturally in vivo, it requires no external source of vibration and thus promises to allow distinction and identification of tissue through noninvasive ultrasonic estimation of the viscoelasticity of arterial wall tissue.

Here we describe our attempt to use the phased tracking method[7,8] to measure simultaneously the pulse wave velocity on both the intimal and adventitial sides of the intact human carotid arterial wall ultrasonically. In this way, we show that blood flow produces small vibration on the surface of the arterial wall and that this vibration propagates from the intima to the adventitia. We also present the results we obtained when attempting to estimate the shear viscoelasticity constant of the human carotid artery wall artery from the frequency characteristics of attenuation during the propagation of vibration.

Vibration caused by blood flow on the intima of the arterial wall

Cardiac pulsation produces changes in the internal pressure on the surface of the arterial wall. Such factors as turbulent flow and eddies caused by the shear stress produced by blood flow are known sources of small vibration at frequencies as high as tens of hertz.[9,10]

Using the phased tracking method[7,8] to measure pulse wave velocity on both the intimal and adventitial sides of the intact wall of the human carotid artery simultaneously with ultrasonography, we found that blood flow produced small vibration ranging from zero to several tens of hertz. Subject A was a 28-year-old healthy male volunteer. Ultrasound was applied in two alternating directions: one perpendicular to the arterial axis, the other about 20° off the arterial axis (Fig. 1). We thus attempted to measure wall vibration and blood flow velocity on both the intimal and adventitial sides of the common carotid artery simultaneously.

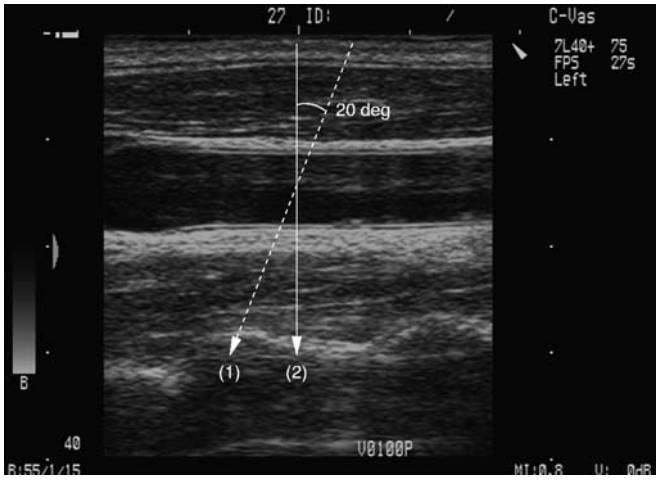

Fig. 1. Cross-sectional B-mode image of the common carotid artery of subject A, a 28-year-old man

Figure 2 shows (1) data obtained on vibration velocity patterns on the intimal side of the posterior wall of the common carotid artery during one cardiac cycle; (2) the vibration velocity pattern on the adventitial side; (3) patterns of blood flow along the axis; (4) patterns of change in the inside diameter of the artery; and (5) the time course of vibration velocity power on the intimal and adventitial sides for each frequency.

When the time course of vibration velocity power for each frequency was followed (Fig. 2d), the frequency was analyzed while moving the 100-ms wide Hanning window in increments of 10 ms. Figure 2 shows that blood flow along the axis was first detected when the pulse wave arrived, and that blood flow velocity increased until the pulse reached the dicrotic notch formed by closure of the aortic valve. Analysis of arterial wall vibration velocity patterns also showed that vibration velocity power was greater from the arrival of the pulse wave (time A in Fig. 2) until the dicrotic notch was formed by closure of the aortic valve (time D) than during other periods.

The large variance in amplitude during the period from pulse wave arrival (time A) seen in Fig. 2 to formation of the dicrotic notch resulting from closure of the aortic valve (time D) is attributable to the change in pressure produced in the artery when blood is ejected from the heart and the aortic valve closes. This change is accompanied by changes in the inside diameter of the artery and distortion changes in the thickness of the arterial wall. During the period B–C, defined as the period between the arrival of a pulse and immediately before the dicrotic notch was formed by closure of the aortic valve, the internal arterial diameter changed little; however, the arterial wall vibration velocity power of the frequency range greater than around 40 Hz was about 10 dB greater than during periods of slower blood flow. Changes in the arterial inner diameter correlated closely with changes in arterial pressure.[3,15] Internal arterial pressure remained essentially constant during period B–C,

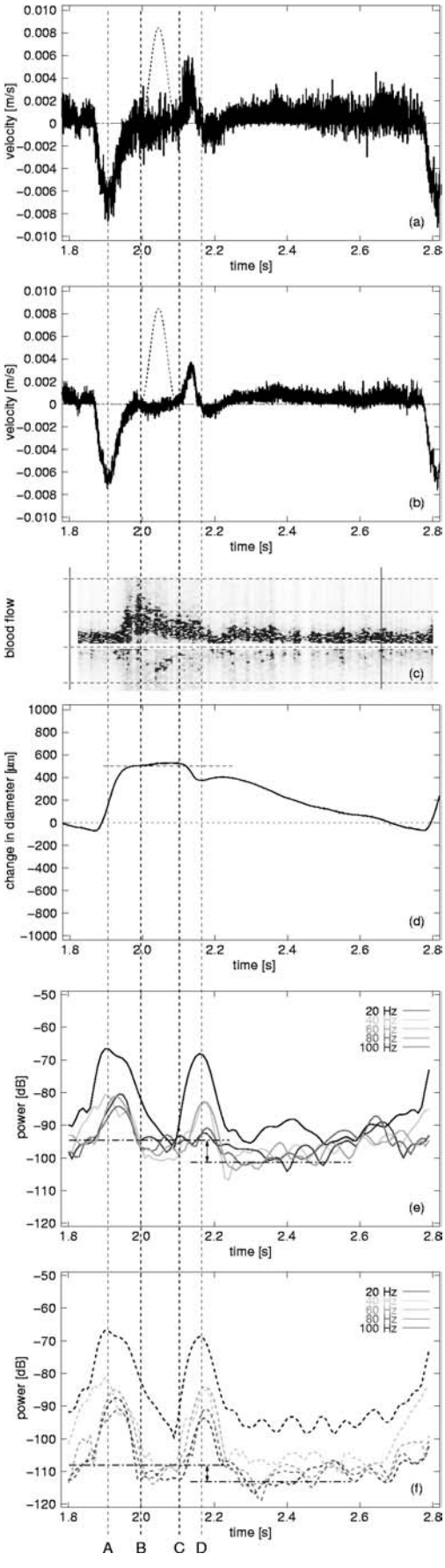

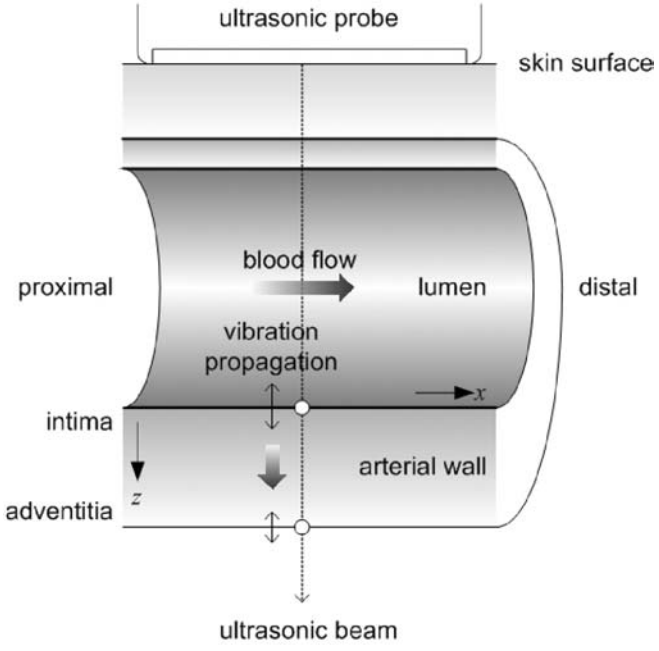

Fig. 3. Measurement of vibration propagation from the intima to the adventitia of the arterial wall

in which the internal diameter of the artery remains almost unchanged. Arterial wall vibration during period B–C may thus be considered attributable solely to blood flow.

Such small vibration caused by blood flow appears to result from both turbulence or eddies associated with the viscosity of blood flowing through the artery and the roughness of the arterial surface.[16] As represented in Fig. 3, the vibration produced on the surface of the arterial wall produces elastic waves, the inner surface of the arterial wall serving as a source of vibration; and this wave is propagated from the intima to the adventitia of the arterial wall.

Measuring the propagation of small vibration from the wall of the human carotid artery

To confirm that the small vibration of frequencies ranging from direct current to tens of hertz produced on the arterial wall is propagated along the axis of the arterial wall, we used ultrasonography to measure small vibration on both the intimal and adventitial sides of the arterial wall simultaneously. We then evaluated the relation between the vibrations recorded. Figure 3 shows two reference points set along the ultrasound beam: one on the intimal side, the other on the adventitial side. The tracking method was used to measure the phased wall vibration at both points simultaneously.[8]

Fig. 2. Vibration of the intima of the posterior arterial wall during a cardiac cycle in subject A. **a, b** Vibration velocity. **c** Axial blood flow. **d** Change in internal diameter of the artery. **e, f** Change in power spectra of vibration velocities

Vibration of the posterior wall of the carotid artery was measured in a healthy 28-years-old male volunteer (subject A) (Fig. 2). During the interval between the pulse wave arrival and the formation of the dicrotic notch resulting from aortic valve closure, the inside diameter of the artery in segment B–C (Fig. 2) changed little, suggesting that arterial pressure remains almost constant and that the vibration produced in this segment is attributable primarily to blood flow.

Wall vibration power on the intimal side differed significantly from that on the adventitial side of the artery when the frequency exceeded 60 Hz, suggesting that the small vibration produced on the surface of the arterial wall is propagated as an elastic wave from the intima to the adventitia while undergoing attenuation through time. This led us to evaluate the correlation between arterial wall vibration on the intimal and adventitial sides after blood is ejected from the heart. We used the amplitude squared coherence function[17,18] to confirm that the small vibration produced on the surface arterial wall by blood flow is propagated from the intimal to the adventitial side.

The amplitude squared coherence function indicates the ratio of power input-based components to output-based components. It is defined from the input signal spectrum $X_i(k)$ and output signal spectrum $Y_i(k)$, as shown below, where E_i denotes the averaging operation.

$$|\gamma(k)|^2 = \frac{E_1\left[X_i^*(k)Y_i(k)\right]^2}{E_i\left[|X_i(k)|^2\right]E_i\left[|Y_i(k)|^2\right]} \quad (1)$$

For example, $|\gamma(k)|^2 = 0.9$ indicates that the power of input-based components makes up 90% of the power of the output signal, and the remaining 10% is noise that cannot be explained by linear propagation of input signals.

Figure 4a shows the data obtained using $|\gamma(f)|^2$ concerning the correlation between carotid artery wall vibration on the intimal and adventitial sides for the period shown in Fig. 2, the Hanning window period, during which blood flow alone seemed to account for the wall vibration velocity patterns observed. The time window interval was set at 100 ms, and data for 10 cardiac beats were averaged in the frequency analysis. Figure 4a shows that coherence was high, in the range of 0 to about 70 Hz. We determined a propagation function for vibration from the intimal to the adventitial side of the arterial wall $H(f)$ and evaluated amplitude and phase characteristics to confirm that vibration produced on the surface of the arterial wall surface was propagated from the intima to the adventitia.

Figure 4b shows the amplitude characteristic $|H(f)|$ of $H(f)$, a function of propagation of vibration from the intimal to the adventitial side of the arterial wall, for the Hanning window period shown in Fig. 2, during which blood flow alone appeared to account for formation of wall vibration velocity patterns. Figure 4c shows data concerning the phase characteristic $\angle H(f)$ obtained in this way.

Figure 4 shows that attenuation of amplitude (Fig. 4b) and delay in phase (Fig. 4c) occurred in the frequency range between about 20 Hz and high coherence at 70 Hz. Here the phase was close to 0 when the frequency was less than about 40 Hz. The pattern of change in the inner diameter of the artery (Fig. 2d), however, showed that the internal diameter of the artery remained almost constant during the interval between the pulse wave arrival caused by ejection and the dicrotic notch formation resulting from closure of the aortic valve, but that the internal diameter increased slowly and slightly before the dicrotic notch was formed.

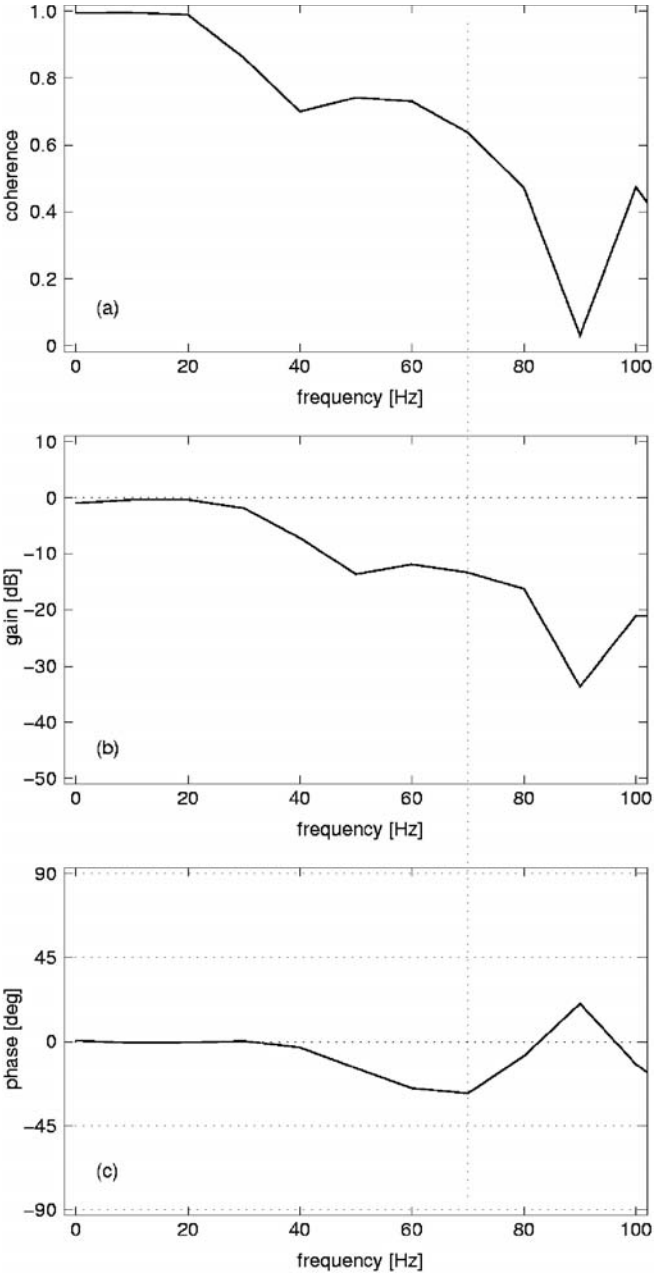

Fig. 4. Frequency characteristics of small vibration between the intima and adventitia of the posterior arterial wall in subject A, a 28-year-old man

These findings combined with the vibration velocity patterns on the intimal and adventitial sides of the arterial wall shown in Fig. 2a,b confirm the production of low-frequency vibration during the period from arrival of the pulse wave

produced by cardiac ejection to formation of the dicrotic notch. Regarding the changes in vibration velocity power on the intimal and adventitial sides of the arterial wall (Fig. 2e,f), we confirmed that the vibration power for the range 40–100 Hz changed little, although that at 20 Hz changed markedly, by about 20 dB. These results suggest that small vibration up to 40 Hz is primarily associated with changes in the inner diameter of the artery resulting from a variation in blood pressure.

In Fig. 4c the calculated phase lag β is 15° at 50 Hz. Elastic wave propagation velocity (c) can thus be obtained using the following equation, assuming that the increase in time-related variation ωt is accompanied by a corresponding increase in dislocation of βx to ωt.[1]

$$c = \mathrm{d}x/\mathrm{d}t = \omega/\beta \tag{2}$$

The vibration propagation velocity c at propagation distance d is equal to 1 mm, the thickness of the arterial wall, and can thus be calculated from the angular frequency ω and phase delay β using the equation $c = \omega/\beta = 1.2$ m/s. These results suggest that the small vibration produced on the surface of the arterial wall by blood flow in the human carotid artery is propagated as shear elastic waves toward the adventitia. They further suggest that the propagation characteristics of the elastic wave transmitted through tissue can be determined from the vibration velocities measured with ultrasonography at multiple points set across the depth of the arterial wall, and that the viscoelasticity characteristics of tissue can be estimated from the propagation characteristics.

Estimation of the shear viscoelasticity constant from the frequency characteristics of attenuation of the shear elastic wave during propagation

The propagation characteristics of shear elastic waves of frequencies less than about 10 kHz are known to vary in frequency when the viscosity of living tissue is taken into account.[11,12] If the shear viscoelasticity constant $\mu = \mu_1 + j\omega\mu_2$ of the Voigt model is applied to the wave function, which takes into account attenuation resulting from viscosity of an elastic body, the following relation is obtained[11,12]

$$\mu = \mu_1 + j\omega\mu_2 = -\frac{\rho\omega}{\gamma^2} \tag{3}$$

where ρ denotes density; μ_1, shear elasticity constant; μ_2, shear viscosity constant; and ω, angular frequency of vibration. The wave number is indicated by γ, taking attenuation into account, and is expressed from the amount of attenuation α and phase β using the equation $\gamma = \alpha + j\beta$.

If $\gamma = \alpha + j\beta$ is applied to Eq. (3) and the real and imaginary terms are rearranged, the shear elasticity constant μ_1 and shear viscosity constant μ_2 can be obtained using the following equations.

$$\begin{cases} \mu_1 = \dfrac{\rho\omega\beta^2\left(\alpha^2-\beta^2\right)^2}{\left(\alpha^2+\beta^2\right)^2} \\ \mu_2 = \dfrac{2\rho\omega\alpha\beta}{\left(\alpha^2+\beta^2\right)^2} \end{cases} \tag{4}$$

Furthermore if $\gamma = \alpha + j\beta$ is applied to Eq. (3), both sides are squared, the real and imaginary parts are rearranged, and the quadratic equation is solved, we can calculate the degree of attenuation α and phase β using the following equations.[11]

$$\begin{cases} \alpha(\omega) = \left(\dfrac{\rho\omega^2\left(\sqrt{\mu_1^2+\omega^2\mu_2^2}-\mu_1\right)}{2\left(\mu_1^2+\omega^2\mu_2^2\right)} \right)^{\frac{1}{2}} \\ \beta(\omega) = \left(\dfrac{\rho\omega^2\left(\sqrt{\mu_1^2+\omega^2\mu_2^2}+\mu_1\right)}{2\left(\mu_1^2+\omega^2\mu_2^2\right)} \right)^{\frac{1}{2}} \end{cases} \tag{5}$$

Assuming that the shear elasticity constant μ_1 and shear viscosity constant μ_2 are constant irrespective of frequency, attenuation α and phase β in Eq. (5) are functions of angular frequency of vibration ω.

The propagation velocity of shear elastic wave c_s can be obtained from the angular frequency ω and phase β of vibration as follows.

$$c_s(\omega) = \frac{\omega}{\beta} = \left(\frac{2\left(\mu_1^2+\omega^2\mu_2^2\right)}{\rho\omega^2\left(\mu_1+\sqrt{\mu_1^2+\omega^2\mu_2^2}\right)} \right)^{\frac{1}{2}} \tag{6}$$

Equation (6) indicates that the propagation velocity of shear elastic wave $c_s(\omega)$ is also a function of angular frequency ω.

Figure 5a–c shows the degree of elastic wave attenuation during propagation α, phase β, and the frequency characteristic of propagation velocity $c_s(\omega)$, calculated using the reported data ($\mu_1 = 2.5$ kPa and $\mu_2 = 15$ Pa·s).[10]

The shear elasticity constant μ_1 and shear viscosity constant μ_2 of soft tissue in vivo can be obtained from the angular frequency ω, the amount of attenuation α, and the phase β of vibration, using Eq. (4).

Because of the thinness of the intact human carotid artery wall (approximately 1 mm), however, simultaneous attenuation α and phase β of vibration during short-distance propagation are often difficult to measure precisely. We therefore devised a method for an approximate estimation of the shear viscoelasticity constant of tissue based on the degree of attenuation, α, during propagation, which is easier to measure than the phase β. Equation (5) can be developed as follows.

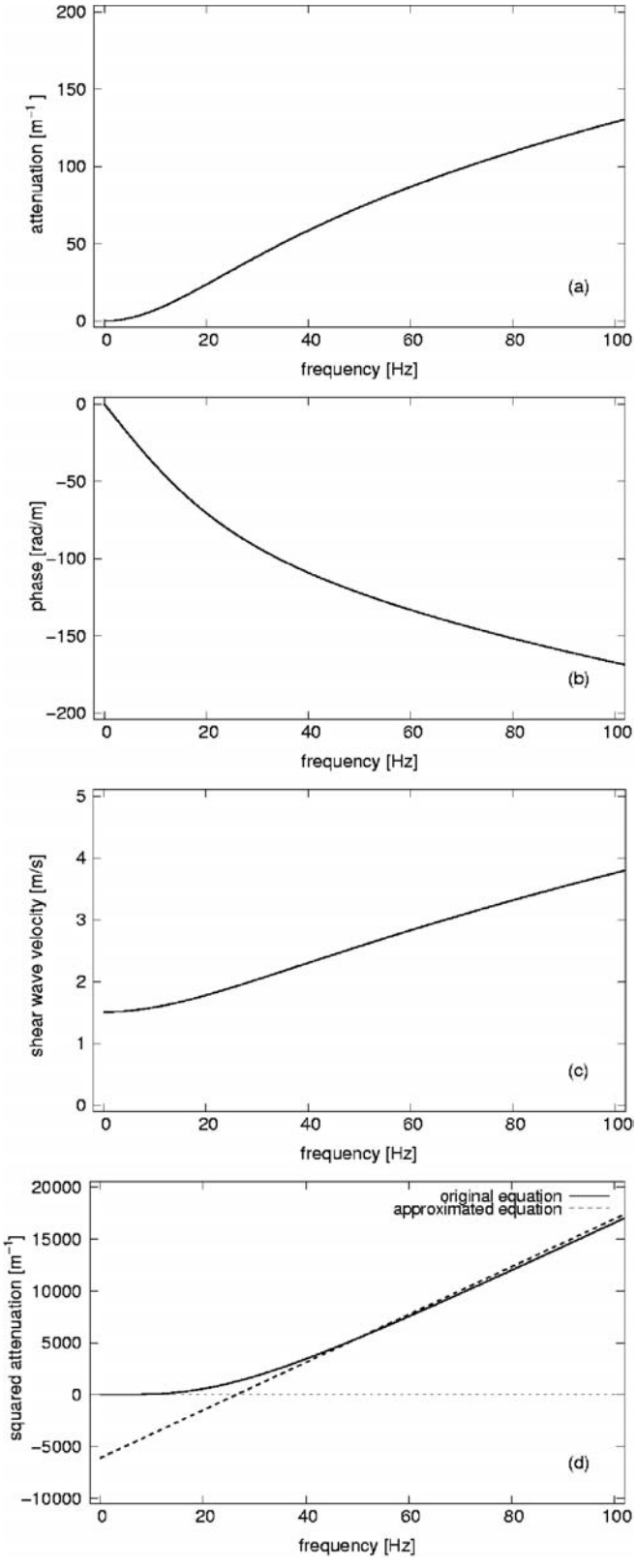

Fig. 5. Frequency characteristics of shear wave propagation: μ_1 = 2.5 kPa, μ_2 = 15 Pa·s

$$\alpha(\omega)^2 = \frac{\rho\omega^2\left(\sqrt{\mu_1^2+\omega^2\mu_2^2}-\mu_1\right)}{2\left(\mu_1^2+\omega^2\mu_2^2\right)} = \rho\omega\mu_2\left\{\left(1+\frac{\mu_1^2}{\omega^2\mu_2^2}\right)^{\frac{1}{2}}-\frac{\mu_1}{\omega\mu_2}\right\}\times\frac{1}{2\mu_2^2}\left(1+\frac{\mu_1^2}{\omega^2\mu_2^2}\right)^{-1}$$

The following equation allows approximation of the high-frequency range, where $\omega^2\mu_2^2 >> \mu_1^2$.

$$\begin{aligned}\hat{\alpha}(\omega)^2 &\approx \frac{\rho\omega}{2\mu_2}\left(1+\frac{\mu_1^2}{2\omega^2\mu_2^2}-\frac{\mu_1}{\omega\mu_2^2}\right)\left(1-\frac{\mu_1^2}{\omega^2\mu_2^2}\right)\\ &\approx \frac{\rho\omega}{2\mu_2}\left(1-\frac{\mu_1}{\omega\mu_2}\right)\\ &\approx \frac{\rho}{2\mu_2}\omega-\frac{\rho\mu_1}{2\mu_2^2}\end{aligned} \tag{8}$$

Assuming that the shear elasticity constant μ_1 and the shear viscosity constant μ_2 remain constant irrespective of frequency, Eq. (8) is converted to a linear function $\hat{\alpha}(\omega)^2 = A\omega + B$, where the first term is the gradient A, and the second is the intercept B. The shear elasticity constant $\hat{\mu}_1$ and shear viscosity constant $\hat{\mu}_2$ can be estimated from coefficients A and B of the first term, ω, using the following equations.

$$\begin{cases}\hat{\mu}_1 = -\dfrac{2\mu_2^2 B}{\rho}\\ \hat{\mu}_2 = -\dfrac{\rho}{2A}\end{cases} \tag{9}$$

Equation (5) can be developed as follows.

$$\alpha(\omega)^2 = \frac{\rho\omega^2\left(\sqrt{\mu_1^2+\omega^2\mu_2^2}-\mu_1\right)}{2\left(\mu_1^2+\omega^2\mu_2^2\right)} = \rho\omega\left\{\left(1+\frac{\omega^2\mu_2^2}{\mu_1^2}\right)^{\frac{1}{2}}-1\right\}\times\frac{1}{2\mu_2^2}\left(1+\frac{\omega^2\mu_2^2}{\mu_1^2}\right)^{-1} \tag{10}$$

and becomes

$$\begin{aligned}\hat{\alpha}(\omega)^2 &\approx \frac{\rho\omega}{2\mu_1}\left(1+\frac{\mu_1^2}{2\omega^2\mu_2^2}-1\right)\left(1-\frac{\omega^2\mu_2^2}{\mu_1^2}\right)\\ &\approx 0\end{aligned} \tag{11}$$

when the angular frequency ω_0 at the point of inflection from Eq. (11) to Eq. (8) can be obtained as follows using Eq. (8)

$$\omega_0 = \frac{\mu_1}{\mu_2} \tag{12}$$

which is the ratio of the shear elasticity constant μ_1 to the shear viscosity constant μ_2.

Figure 5d shows the frequency characteristic of the square of shear elastic wave attenuation calculated using

data reported by Oestreicher (μ_1 = 2.5 kPa, μ_2 = 15 Pa·s).[11] The same parameter was estimated by our method using an approximation with the linear function of angular velocity ω. Figure 5d shows that this method, using the approximation with a linear function of angular frequency ω, is valid for the frequency range in which $\omega^2\mu_2^2 >> \mu_1^2$. The point of inflection of the frequency characteristic of squared shear elastic wave attenuation is shown to be close to the ratio of the elasticity constant μ_1 to the shear viscosity constant μ_2 (i.e., f_0 = 26.5 Hz).

Shear viscoelasticity constant estimated from the propagation attenuation frequency characteristics of human carotid artery wall vibration

Regarding the vibration on the intimal and adventitial sides of the human carotid artery wall measured simultaneously by ultrasonography (Fig. 2), the data obtained concerning the amplitude and phase characteristics of the amplitude squared coherence function and the propagation function (Fig. 4) show that vibration produced by blood flow is linearly propagated toward the adventitial side and is attenuated over time. This suggests that arterial wall tissue can be deemed a Voigt model when analyzing the propagation characteristics of the vibration produced on the surface of the arterial wall. We thus attempted to estimate shear elasticity constant μ_1 and shear viscosity constant μ_2 from the frequency characteristics of the attenuation of vibration during propagation from the intimal to the adventitial side of the human arterial wall using Eq. (8).

From ΔZ_{mn}, which denotes the distance between the intima *m* and the adventitia *n*, corresponding to the thickness of the arterial wall, the frequency characteristic $\alpha_{mn}(f)^2$ of vibration power per unit length between point *m* and point *n* can be obtained using the following equation.

$$\alpha_{mn}(f)^2 = \frac{|H(f)|^2}{\Delta Z_{mn}} \tag{13}$$

Then, to apply the approximation Eq. (8) to the high-frequency range ($\omega^2\mu_2^2 >> \mu_1^2$), we selected a frequency range over which vibration appears to be propagated from the intima to the adventitia of the arterial wall. Applying the amplitude squared coherence function for the period starting some time after cardiac ejection and ending immediately before closure of the aortic valve causes the dicrotic notch to form (i.e., the period during which small vibration appears to result from blood flow alone). Attenuation of vibration during propagation over the selected range is squared and analyzed using the least-squares method to obtain gradient *A* and intercept *B* of the linear function. We then used Eq. (8) to estimate the shear elasticity constant μ_1 and shear viscosity.

This method was applied to the carotid artery of a healthy 28-year-old male volunteer. Figure 6 shows the data we obtained concerning coherence of wall vibration velocity on the intimal and adventitial sides of the posterior wall of the carotid artery (Fig. 6a) and the squared attenuation of vibration during propagation from the intimal to the adventitial side of the posterior wall of the carotid artery (Fig. 6b).

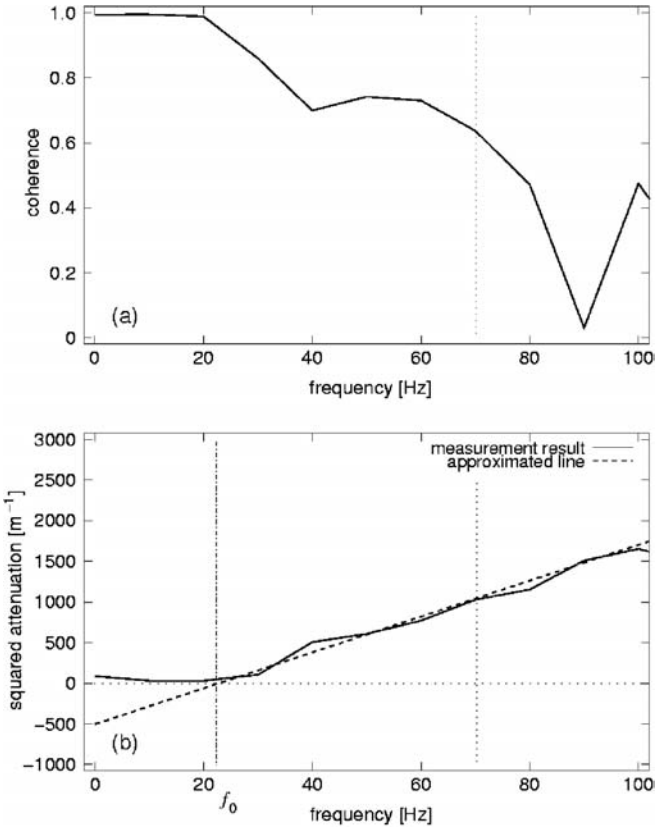

Fig. 6. Frequency characteristics of small vibration between the intima and adventitia of the posterior arterial wall of subject A

Squared attenuation increased linearly with frequency over the approximate range of about 30–100 Hz (Fig. 6b) and was subjected to least-squares analysis (Fig. 6a) over the range of 30–70 Hz, corresponding to the range with high coherence of vibration on the intimal and adventitial sides. The approximation line thus obtained gave $\hat{\mu}_2$ = 156 Pa·s using the shear viscoelasticity constant obtained from this line by Eq. (8). Considering the ratio of the thus determined shear elasticity constant μ_1 and the shear viscosity constant μ_2, the point of inflection of the frequency characteristic of squared attenuation was found to be close to 23 Hz.

We attempted to estimate the shear viscoelasticity constant in two other healthy male volunteers (subjects B and C, both 21 years old) in the same way for the period starting shortly after the pulse produced by cardiac ejection arrived and ending immediately before the dicrotic notch formed as a result of closure of the aortic valve – the period during which blood flow alone appears to account for the vibration.

Figure 7 shows the data collected from subject B concerning wall vibration velocity coherence on the intimal and adventitial sides of the carotid artery (Fig. 7a) and the squared attenuation of the vibration propagated from the intimal to the adventitial side of the posterior wall of

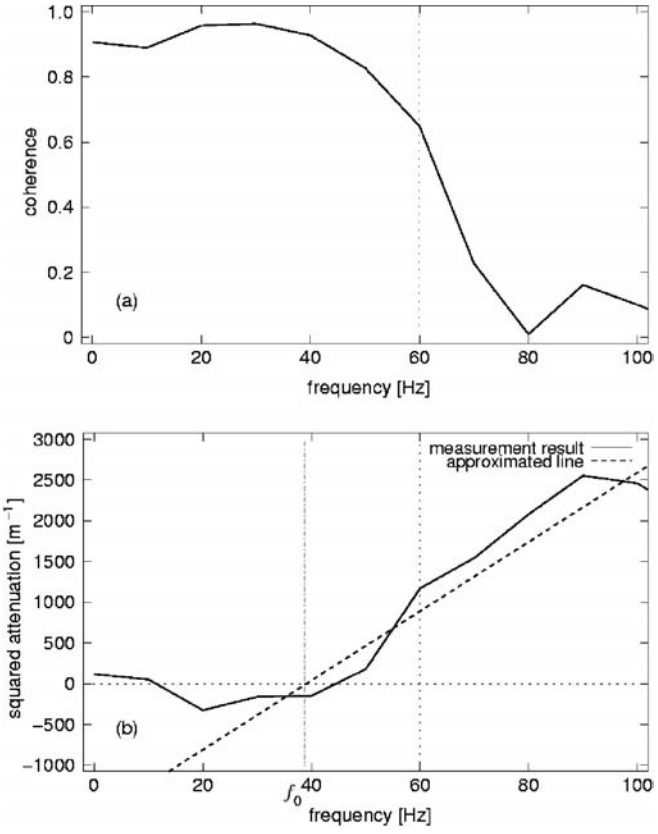

Fig. 7. Frequency characteristics of small vibration between the intima and adventitia of the posterior arterial wall of subject B, a 21-year-old man

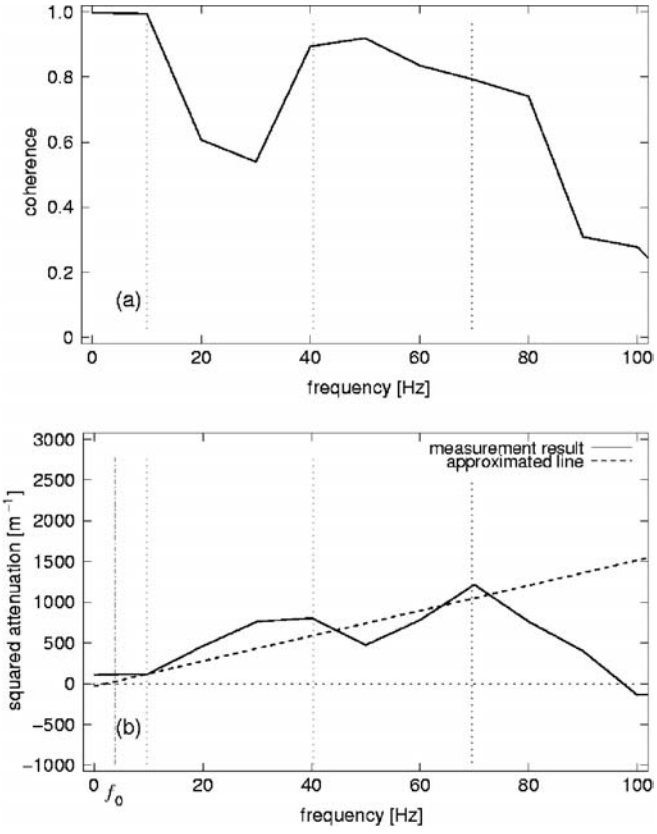

Fig. 8. Frequency characteristics of small vibration between the intima and adventitia of the posterior arterial wall of subject C, a 21-year-old mean

the carotid artery (Fig. 7b). Figure 7b shows that squared attenuation increased linearly with a frequency of about 40–90 Hz. The frequency range of about 40–60 Hz with high coherence of vibration on the intimal and adventitial sides was subjected to least-squares analysis to determine the shear viscoelasticity constant, yielding $\hat{\mu}_1 = 19\,\text{kPa}$ and $\hat{\mu}_2 = 81\,\text{Pa}\cdot\text{s}$. The point of inflection of squared attenuation was close to 37 Hz.

Figure 8 shows the data obtained from subject C, a 21-year-old man, concerning coherence of wall vibration velocity on the intimal and adventitial sides of the carotid artery (Fig. 8a) and squared attenuation of vibration propagated from the intimal to the adventitial sides of the posterior wall of the carotid artery (Fig. 8b). Coherence was low over the frequency range of about 20–30 Hz (Fig. 8a). Analysis of the frequency characteristics of squared attenuation revealed a dip at about 30 Hz (Fig. 8b).

Equation (8) was applied to the frequency range of about 40–80 Hz, where the coherence of vibration on the intimal and adventitial sides was high. The shear viscoelasticity constants thus obtained were $\hat{\mu}_1 = 2.9\,\text{kPa}$ and $\hat{\mu}_2 = 223\,\text{Pa}\cdot\text{s}$. The point of inflection of the frequency characteristic of squared attenuation was around 2 Hz.

These results indicate that blood flow induces small vibration on the arterial wall of the human carotid artery and that this vibration is propagated from the intima to the adventitia of the arterial wall. The use of frequency characteristics of attenuation of vibration during propagation are likely to facilitate estimation of the shear viscoelasticity constant of arterial wall tissue. Also, when coherence is low over part of the frequency range, as seen with subject C, we may be able to estimate the shear viscoelasticity constant of arterial wall tissue using the frequency characteristic of attenuation of vibration for another frequency range with high coherence.

As shown in Fig. 8b, the linear approximation curve dipped at about 30–40 Hz. When the curve was derived from the 50- to 80-Hz frequency range, however, the shear elasticity constant was $\hat{\mu}_1 = 22\,\text{kPa}$, and the shear viscosity constant was $\hat{\mu}_2 = 93\,\text{Pa}\cdot\text{s}$. These results suggest that vibration differs from the propagation of an elastic wave in that oscillation may occur around the 40-Hz region. We plan to use these findings to analyze the mode of vibration of the arterial wall.

Conclusions

We used the phased tracking method to measure simultaneously the wall vibration on the intimal and adventitial sides of the human carotid artery with ultrasonography. We

also conducted frequency analysis of wall vibration velocity patterns, including an evaluation of the association between the intimal and adventitial sides over specific ranges of small vibration frequency. The analysis showed that small vibration of up to about 100 Hz occurred on the surface of the arterial wall, and that the vibration was propagated from the intimal to the adventitial side of the artery.

We also attempted to estimate the shear viscoelasticity constant of tissue from the propagation characteristics of this shear elastic wave and proposed a method for estimating the viscoelasticity characteristics on the basis of attenuation of the shear elastic wave alone by frequency characteristics. We then attempted to use this method to estimate the shear elasticity and shear viscosity constants of the arterial wall.

Our results suggest the possibility of distinguishing and identifying tissue based on the propagation characteristics of arterial wall vibration using percutaneous ultrasonography and an internal source of vibration inherent in vivo (i.e., the vibration produced by the flow of blood through the arteries). This method requires no extracorporeal source of vibration or other means of stress measurement required by conventional methods used to measure viscoelasticity. Ultrasound measurement alone suffices. This method seems to be particularly useful for studying the arterial wall, where the propagation distance is short, and precise simultaneous measurements of the propagation time and changes in phase and attenuation is difficult. We plan to continue to study the morphologic features of elastic wave propagation through the arterial wall and to estimate the shear viscoelasticity characteristics in vivo.

This study was conducted within the framework of the research and development program of the Japan Society of Ultrasonics in Medicine.

References

1. Hallck P. Arterial elasticity in man in relation to age as evaluated by the pulse wave velocity methods. Arch Intern Med 1970;85: 742–60.
2. Imura T, Yamamoto K, Kanamori K, et al. Non-invasive ultrasonic measurement of the elastic properties of the human abdominal aorta. Cardiovasc Res 1986;20:208–14.
3. Li K-JJ. Arterial system dynamics. New York: New York University Press, 1987. p. 47–90.
4. Gow BS, Taylor MG. Measurement of viscoelastic properties of arteries in the living dog. Circ Res 1968;23:112–22.
5. Cox RH. Determination of the true phase velocity of arterial pressure waves in vivo. Circ Res 1971;29:407–18.
6. Kodama T, Takahashi K, Shibuya M. Vascular biology. Tokyo: Kodansha, 1997. p. 37–59 (in Japanese).
7. Kanai H, Koiwa Y. Real-time velocimetry for evaluation of change in thickness of arterial wall. Ultrasonics 2000;38:381–6.
8. Kanai H, Sato M, Koiwa Y, et al. Transcutaneous measurement and spectrum analysis of heart wall vibrations. IEEE Trans UFFC 1996;43:791–810.
9. Plett MI, Beach KW, Dunmire B, et al. In vivo ultrasonic measurement of tissue vibration at a stenosis: a case study. Ultrasound Med Biol 2001;27:1049–58.
10. Sunagawa K, Kanai H, Koiwa Y, et al. Simultaneous measurement of vibrations on arterial wall upstream and downstream of arteriostenosis lesion and their analysis (translation). J Med Ultrasonics 2001;28:157–73.
11. Oestreicher HL. Field and impedance of an oscillating sphere in a viscoelastic medium with an application to biophysics. J Acoust Soc Am 1951;37:707–14.
12. Yamakoshi Y, Sato J, Sato T. Ultrasonic imaging of internal vibration of soft tissue under forced vibration. IEEE Trans UFFC 1990;37:45–53.
13. Catheline S, Wu F, Fink M. A solution to diffraction biases in sonoelasticity: the acoustic impulse technique. J Acoust Soc Am 1999;105: 2941–50.
14. Catheline S, Thomas J, Wu F, et al. Diffraction field of a low frequency vibrator in soft tissues using transient elastography. IEEE Trans UFFC 1999;46:1013–9.
15. Sugawara M, Niki K, Furuhata H, et al. Relationship between the pressure and diameter of the carotid artery in humans. Heart Vessels 2000;15:49–51.
16. Hino M. Introduction to fluid mechanics. Tokyo: Asakura Shoten; 1992. p. 301–18 (in Japanese).
17. Kanai H. Spectrum analysis of sound and vibration. Tokyo: Corona Publishing; 1999. p. 256–75 (in Japanese).
18. Hino M. Spectral analysis. Tokyo: Asakura Shoten; 1977. p. 63–5.